


METEOROLOGY

Assessing the Moist and Dry Static Energies in the Atmosphere as a Van Der Waals Gas in 2015 and 2017 over the Metropolitan Region of Natal-RN, Brazil

Avaliação das Energias Estáticas Úmidas e Secas na Atmosfera como Gás de Van Der Waals em 2015 e 2017 sobre a Região Metropolitana de Natal-RN, Brasil

Deusdedit Monteiro Medeiros¹ , Isamara de Mendonça Silva^{1,2}  & David Mendes² 

¹ Universidade Federal do Rio Grande do Norte, Programa de Pós-Graduação em Engenharia Aeroespacial, Laboratório de Pesquisas Atmosféricas, Lagoa Nova, Natal, RN, Brasil

² Universidade Federal do Rio Grande do Norte, Programa de Pós-Graduação em Ciências Climáticas, Lagoa Nova, Natal, RN, Brasil
E-mails: kalbramond@gmail.com; isamara.mendonca.s@gmail.com; david.mendes22@gmail.com

Abstract

This study evaluated the monthly average of the enthalpy, geopotential, latent heat content, moist static energy, and dry static energy at several levels of the atmosphere as a Van Der Waals gas from radiosonde data at 00:00 UTC and 12:00 UTC over the metropolitan region of Natal-RN-Brazil. The years 2015 and 2017 were considered because they presented more than 70% of complete data, with days coinciding at both times. To construct the vertical profiles of the variables, the density, specific humidity, and geopotential were calculated at each level through a mathematical approximation based on the Calculus. The Van der Waals-like atmosphere results showed that the latent heat content compensated for any change in enthalpy and potential energy from the surface to the mid-troposphere. Energy was exchanged among enthalpy, geopotential, and latent heat content, showing a roughly constant moist static energy. The moist static energy was a conserved quantity under adiabatic and hydrostatic transformations, although the dry static energy was not conserved. The results of the atmosphere as a Van Der Waals gas and the atmosphere as an ideal gas were compared, proving to be similar.

Keywords: Enthalpy; Geopotential; Latent heat

Resumo

Esse estudo avaliou a média mensal de entalpia, geopotencial, conteúdo de calor latente, energia estática úmida e energia estática seca em vários níveis de uma atmosfera como gás de Van der Waals, a partir de dados de radiossonda às 00:00 UTC e 12:00 UTC na região metropolitana de Natal-RN-Brasil. Foram considerados os anos de 2015 e 2017 por apresentarem mais de 70% de dados completos, com dias coincidentes em ambos os horários. Foram calculados a densidade, a umidade específica e o geopotencial em cada nível através de uma aproximação matemática baseada no Cálculo Diferencial e Integral, para a construção dos perfis verticais das variáveis. Os resultados da atmosfera do tipo Van der Waals mostraram que o conteúdo de calor latente compensou qualquer mudança na entalpia e na energia potencial da superfície para a média troposfera. Energia foi trocada entre entalpia, geopotencial e calor latente, mostrando uma energia estática úmida aproximadamente constante. A energia estática úmida foi conservada sob transformações adiabáticas e hidrostáticas, embora a energia estática seca não tenha sido conservada. Os resultados da atmosfera como gás Van Der Waals e da atmosfera como gás ideal foram comparados, mostrando-se semelhantes.

Palavras-chave: Entalpia; Geopotencial; Calor latente

1 Introduction

Thermodynamics is an essential way of understanding the quantitative properties of the atmosphere. Some fundamental ideas and relationships in thermodynamics are introduced to study atmospheric phenomena. For example, pressure, volume, and temperature, can be related by a mathematical expression called an equation of state. Numerous scientific studies have utilized the ideal gas equation of state to analyze thermodynamics in the atmosphere since the air is made up of gases, which individually obey the ideal gas law (Holton 2004; Wallace & Hobbs 2006). Several works have studied geopotential, temperature, water vapor, and other variables based on radiosonde observations and reports for the atmosphere as an ideal gas (Smith, Woolf & Jacob 1970; Chouinard & Staniforth 1995; Marshall 2002; Laroche & Sarrazin 2013; Qian et al. 2018; Ermakov et al. 2021.)

The Van der Waals equation considers the intermolecular interactions of gas constituents. It depends on pressure, volume, temperature, and molar gas constant, presenting two constants determined from the critical point in the pressure-volume function diagram (Van der Waals 1873, apud Nussenzveig 2000). Besides, the critical properties (critical temperature and critical pressure) of a gas mixture are obtained through the group contribution method, and pseudocritical parameters resulting from the linear mixtures rule, known as the Kay Rule (Daubert 1989; Jalowka 1986; Kay 1936, apud Joback 1987). Silva, Silva & Medeiros (2019) analyzed the atmosphere from radiosonde data, finding a difference between the densities in the atmosphere as a Van der Waals gas and an ideal gas. Medeiros, Silva & Silva (2020) proposed a Van der Waals-like form state equation for the atmosphere and computed corrections in the alternative form of the first law of thermodynamics and the virtual temperature. Moreover, Bolton (1980) calculated the potential temperature non-conventionally, even though the atmosphere was assumed to be an ideal gas in this study.

The moist static energy MSE is the conserved atmospheric thermodynamic property during adiabatic or pseudoadiabatic ascent or descent with water undergoing transitions between liquid and vapor phases. It depends on specific heat at constant pressure, the temperature of the air parcel, geopotential, latent heat of vaporization, and specific humidity (Wallace & Hobbs 2006). In energy terms, MSE is the sum of dry static energy (DSE) (the enthalpy per unit mass ($c_p T$) plus potential energy (Φ)) and latent heat content ($L_v q$). The MSE could indicate atmospheric stability and energy available for convective processes. Recent work has

shown that tropical atmospheric dynamics force the sub-cloud moist static energy over land and ocean in the tropics to be very similar in regions of deep convection (Zhang & Fueglistaler 2020). In turn, Yano & Ambaum (2017) used approximate formulae of MSE to present that the temperature dependence of latent heat must be considered.

The metropolitan region of Natal (MRN) is in a tropical area adjacent to the Atlantic Ocean, where atmospheric convection plays an important role in cloud formation and precipitation. Assessing the vertical profile of MSE is essential to better understanding the region's atmospheric dynamics, especially convective processes and climate variability. In this context, a thermodynamic process of saturated air lifted dry adiabatically was analyzed, using an unusual approach to determine how energy exchanges. Hence, the present work evaluated the nocturnal and diurnal vertical profiles of the monthly average of $c_p T$, Φ , $L_v q$, MSE , and DSE per unit mass of the atmosphere as a Van Der Waals Gas. The radiosonde data at 00:00 UTC and 12:00 UTC for 2015 and 2017 over the metropolitan region of Natal (MRN) in Rio Grande do Norte, Brazil, were used. To better understand the results, the atmosphere as a Van Der Waals gas and the atmosphere as an ideal gas were compared.

2 Methodology and Data

The city of Natal is located on the eastern coast of northeast Brazil (NEB) and is washed by the Atlantic Ocean. Natal has an area of 167,401 km^2 and an estimated 896,708 inhabitants (IBGE 2021). This city has a tropical climate with dry summers. The dry and intense season occurs during the interval from Spring to Summer, and the rainy season is concentrated from Autumn to Winter (Alvares, Stape & Sentelhas 2014).

This study uses the Wyoming Weather Web dataset of the Department of Atmospheric Science of the College of Engineering and Physical Sciences of the University of Wyoming (<https://weather.uwyo.edu/upperair/sounding.html>). The data used are the daily pressure values, temperature, and relative humidity measured by the radiosonde at 00:00 UTC and 12:00 UTC for 2015 and 2017 in the atmosphere over the MRN, located on the eastern coast of the NEB (Figure 1). The years 2015 and 2017 were chosen because they presented more than 70% of complete data, whose days coincided at 00:00 UTC and 12:00 UTC. Subsequently, the data are interpolated to the values corresponding to regularly spaced altitudes $z_i (i = 1, 2, 3, \dots, n)$ every ten meters, from $z_0 = 50 \text{ m}$ to a height $z_n = 10000 \text{ m}$.

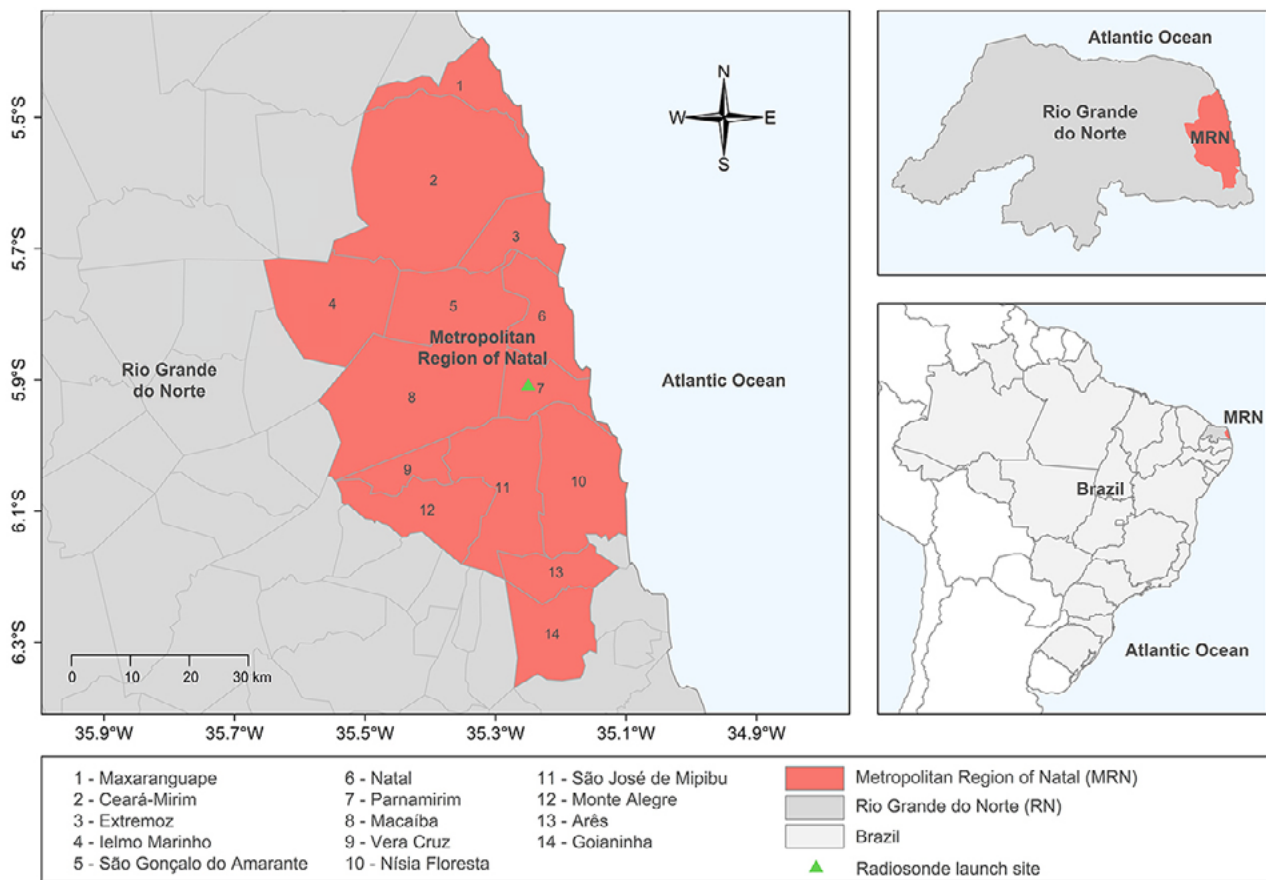


Figure 1 Metropolitan Region of Natal (MRN - orange at the left top), located in Rio Grande do Norte State (gray at the right top), east coast of Brazil (light gray at the right top). The MRN comprises 14 cities, numbered 1 to 14, in the top left corner and named at the bottom. The green triangle at the left top indicates the radiosonde launch site.

From Tetens's empirical equation (Tetens 1930, apud Huang 2018) and the definition of relative humidity and the percentage water content (Wallace & Hobbs 2006), the concentration of the water $C_{\%i}$ is calculated at each z_i by Equation 1,

$$C_{\%i} = 610.8 \frac{RH_i}{p_i} \exp \left[\frac{17.3t_i}{237.3 + t_i} \right] \quad (1)$$

where RH_i is the relative humidity in %, p_i is the pressure of air in Pa, and t_i is the temperature in °C. The analytical equation is shown in Rogers & Yau (1996). The critical temperature T_{Ci} and critical pressure P_{Ci} are then computed through the Kay rule, and the corresponding values of the concentration of the water $C_{\%i}$, calculated by Equation 1 using Table 1.

Following, the values of the Van der Waals constants a_i and b_i are computed at each regular height z_i . Further math details can be seen in Silva, Silva & Medeiros (2019) and

Medeiros, Silva & Silva (2020). From the Van der Waals equation, as seen in Equation 2 (Van der Waals 1873, apud Nussenzveig 2000),

$$\left[p_i + a_i \left(\frac{n_i}{V_i} \right)^2 \right] [V_i - n_i b_i] = n_i R^* T_i \quad (2)$$

and the interpolated pressures p_i and temperatures T_i , the atmospheric densities ρ_i at each point z_i is determined through Equation 3,

$$\rho_i^3 - \frac{1}{b_i} \rho_i^2 + \frac{R^* T_i + p_i b_i}{a_i b_i} \rho_i - \frac{p_i}{a_i b_i} = 0 \quad (3)$$

where the universal gas constant $R^* = 8.3145 \text{ JK}^{-1} \text{ mol}^{-1}$, and the definition $\rho_i \equiv n_i / V_i (\text{mol m}^{-3})$ is used. Here, n_i and V_i correspond to the number of moles and volume at each altitude z_i . Two roots for each ρ_i of Equation 3 are complex numbers, and one is a real number. Therefore, the densities

ρ_i of the Van der Waals-like atmosphere are calculated using the real solution at each height, which is the one that has physical significance. The results are then multiplied by molar mass M (Table 1) to obtain the densities in gm^{-3} .

From the ideal gas equation (Wallace & Hobbs 2006) (Equation 4),

$$p_i V_i = n_i R^* T_i \quad (4)$$

the atmospheric densities ρ_i at each point z_i is determined through Equation 5

$$\rho_i = \frac{p_i}{R^* T_i} = 0 \quad (5)$$

where $R^* = 8.3145 JK^{-1} mol^{-1}$, p_i is the pressure of air in Pa , T_i is the temperature in K , n_i is the number of moles, V_i is the volume, and $\rho_i \equiv n_i/V_i (mol m^{-3})$.

Combining the pressure due to water vapor, relative humidity, specific humidity, and Teten's empirical equation

(Wallace & Hobbs 2006; Tetens 1930, apud Huang 2018), the specific humidity q_i at each regular height z_i is computed by Equation 6,

$$q_i = \frac{\varepsilon RH_i [6.108 \exp(17.3 t_i / (237.3 + t_i))]}{p_i + [6.108 \exp(17.3 t_i / (237.3 + t_i))] RH_i (\varepsilon - 1)} \quad (6)$$

where $\varepsilon = 0.622$, RH_i is the relative humidity in %, p_i is the air pressure in Pa , and t_i is the air temperature in $^{\circ}C$.

From Calculus, the definite integral of $f(x)$ from c to d is described in Equation 7 as

$$\int_c^d f(x) dx = \lim_{n \rightarrow \infty} \sum_{i=1}^n f(x_i^*) \Delta x \quad (7)$$

provided that this limit exists and gives the same value for all possible choices of sample points x_i^* (Stewart 2016). The function $f(x)$ is defined in the interval $[c, d]$, which is divided into n subintervals of equal width $\Delta x = (d - c)/n$. Let x_i^* ($i = 0, 1, 2, 3, \dots$) be any sample points in these subintervals, so x_i^* lies in the i th subinterval $[x_{i-1}, x_i]$.

Table 1 Critical parameters and the atmospheric composition (Internet Archive 2010; NASA 2021).

Chemical Compound	$T_c(K)$	$P_c(Bar)$	Concentration (%)
Nitrogen (N_2)	126.20	34.00	78.084
Oxygen (O_2)	154.60	50.43	20.946
Argon	150.90	48.98	0.934
Carbon Dioxide	304.20	73.83	0.0314
Neon	44.44	27.20	0.001818
Methane	190.60	45.99	0.0002
Helium	5.20	2.28	0.000524
Krypton	209.40	55.02	0.000114
Hydrogen	33.19	13.13	0.00005
Ozone	261.05	55.32	0.000007
Xenon	289.70	58.40	0.0000087
Nitrous Oxide	309.60	72.45	0.00003
Nitrogen Dioxide	430.75	78.84	0.000002
Iodine	819.15	117.00	0.000001
Carbon Monoxide	132.90	34.99	0.00001
Water	647.10	220.55	$C_{\%}$
Air ($N_2 + O_2$)	132.2	37.45	99.9982
Outcome	T_c	P_c	$M (gmol^{-1})$
Dry Air	132.4335	37.5937	28.9645
Moist Air ($C_{\%}$)	T_c to $C_{\%}$	P_c to $C_{\%}$	M to $C_{\%}$

The variation of geopotential (Equation 8), from sea level ($z = 0$) to height z , gives the geopotential,

$$\Phi(z) = - \int_0^z \frac{dp}{\rho} \quad (8)$$

where $\Phi(0)$ is set to zero at sea level, p is the pressure and ρ is the density (Wallace & Hobbs 2006). Dealing with the atmosphere's density in meteorology is not convenient since it generally is not a measured quantity. Consequently, the geopotential given in Equation 8 cannot be calculated.

Therefore, based on the description of the definite integral (Equation 7), this work uses an approximation to calculate the geopotential (Equation 8) from the density (Equation 3, for the Van der Waals-like atmosphere, and Equation 5, for the atmosphere as an ideal gas) computed at altitudes z_i ($i = 0, 1, 2, 3, \dots$), with n points sufficiently large from $z_0 = 50 \text{ m}$ to height $z_n = 10000 \text{ m}$. In this new approach, the geopotential at each point z_i is written as seen in Equation 9,

$$\begin{aligned} \Phi_i = \Phi(z_i) &= - \int_0^z \frac{dp_i}{\rho_i} \cong - \sum_{i=0}^z \frac{\Delta p_i}{\rho_i} = - \sum_{i=0}^z \frac{p_{i+1} - p_i}{\rho_i} \\ \Phi_i &\equiv \sum_{i=0}^z \frac{p_i - p_{i+1}}{\rho_i} \end{aligned} \quad (9)$$

where p_0 is the pressure at the lower level ($z_0 = 50 \text{ m}$) near the sea, p_i and ρ_i correspond to the pressure and density at each altitude z_i , and $\Delta p_i \equiv p_{i+1} - p_i$.

The moist static energy (MSE) is the conserved quantity during adiabatic or pseudoadiabatic ascent or descent with water undergoing transitions between liquid and vapor phases, which is defined by the sum of the enthalpy per unit mass of air ($c_p T$), the gravitational potential (Φ), and the latent heat content ($L_v q$) (Wallace & Hobbs 2006). Here, T is the temperature of the air parcel, and is the specific humidity. From this, the moist static energy at each altitude z_i (MSE_i) was computed by

$$MSE_i = c_p T_i + \Phi_i + L_v q_i \quad (10)$$

where $c_p = 1004 \text{ J K}^{-1} \text{ kg}^{-1}$ is the heat capacity of air and $L_v = 2.25 \times 10^6 \text{ J kg}^{-1}$ is the latent heat of vaporization of water. Here, T_i is the temperature of the air parcel, Φ_i is the gravitational potential (calculated by Equation 6), and q_i is the specific humidity (calculated by Equation 9) at each point z_i . The sum of the first and second terms in Equation 10 is called the dry static energy (DSE_i).

3 Results

Figure 2 presents the monthly average enthalpy ($c_p T$), geopotential (Φ), latent heat content ($L_v q$), moist static energy (MSE), and dry static energy (DSE) from 50 m to 10 km at 00:00 UTC and 12:00 UTC for the atmosphere as a Van Der Waals during the year over the MRN, where all energy values are multiplied by the power 10^3 and in units of J/kg . Enthalpy decreases from $300 \times 10^3 \text{ J/kg}$ to $240 \times 10^3 \text{ J/kg}$ (Figures 2A and 2F), geopotential increases from $5 \times 10^3 \text{ J/kg}$ to $95 \times 10^3 \text{ J/kg}$ (Figures 2B and 2G), and latent heat content decreases from $36 \times 10^3 \text{ J/kg}$ to 0 (Figures 2C and 2H), from low to mid-troposphere in both times. Therefore, enthalpy contributes considerably to moist static energy at the nocturnal and diurnal times, collaborating from 88% ($\sim 0.2 \text{ km}$) to 72% ($\sim 9.7 \text{ km}$). Furthermore, geopotential and latent heat content contribute to moist static energy from 2% ($\sim 0.2 \text{ km}$) to 28% ($\sim 9.7 \text{ km}$) and from 10% ($\sim 0.2 \text{ km}$) to 0% ($\sim 6.0 \text{ km}$), respectively.

Enthalpy and geopotential showed regularity in the energy values at each level (Figures 2A, 2B, 2F, and 2G), implying uniformity in the dry static energy at each height from January to December (Figures 2E and 2J). The latent heat content presented minor and chaotic variations between 1 km and 6 km (Figures 2C and 2H), implying a short decrease in the moist static energy during the year (Figures 2D and 2I). The dry static energy was increased by approximately $36 \times 10^3 \text{ J/kg}$ from 50 m to 10.0 km because enthalpy decreased by $60 \times 10^3 \text{ J/kg}$ and geopotential increased by $95 \times 10^3 \text{ J/kg}$ (Figures 2A, 2B, 2C, 2F, 2G, and 2H) from 50 m to 10.0 km. The latent heat content was decreased by approximately $36 \times 10^3 \text{ J/kg}$ in the troposphere (Figures 2C and 2H). In general, the latent heat content compensated for any change in enthalpy and potential energy. From 50 m to 7.0 km, the moist static energy was maintained equal to the dry static energy plus latent heat content. Still, it was only equal to the dry static energy from 7 km to 10.0 km, where no latent heat content existed. Thus, energy was exchanged among enthalpy, geopotential, and latent heat content for the saturated air lifted dry adiabatically, showing a nearly constant moist static energy. Therefore, the moist static energy was a conserved quantity under adiabatic and hydrostatic transformations. Except for some close results near the surface, the outcomes were identical at 00:00 UTC and 12:00 UTC.

Figure 3 shows the monthly average enthalpy ($c_p T$), geopotential (Φ), latent heat content ($L_v q$), moist static energy (MSE), and dry static energy (DSE) from 50 m to 1.5 km at 00:00 UTC and 12:00 UTC for the atmosphere as a Van Der Waals during the year over the MRN, where all energy values are multiplied by the power 10^3 and in

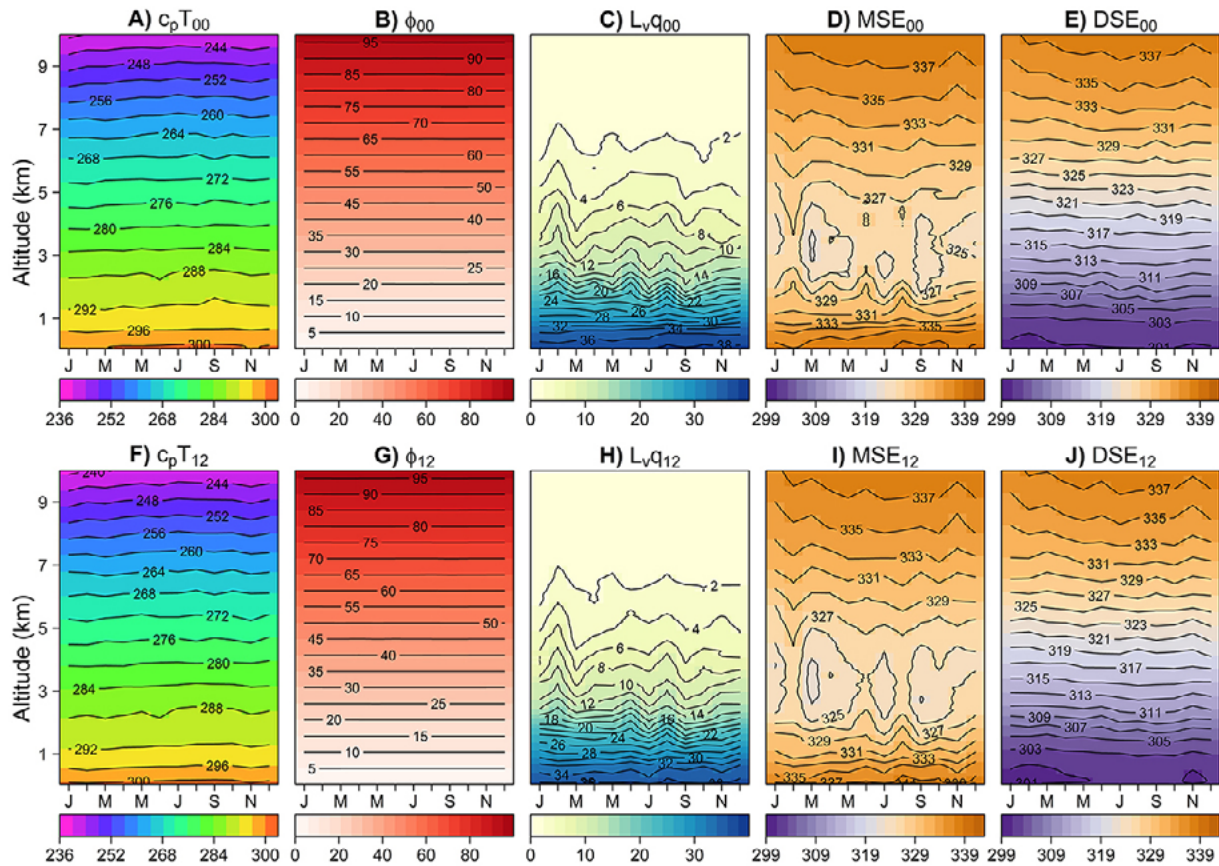


Figure 2 Vertical profiles of the atmosphere as a Van Der Waals gas for the years 2015 and 2017 over the MRN. Monthly average at 00:00 UTC (variables on top with indices 00): A. Enthalpy ($c_p T_{00}$); B. Geopotential (Φ_{00}); C. Latent heat content ($L_v q_{00}$); D. Moist static energy (MSE_{00}); E. Dry static energy (DSE_{00}). Monthly average at 12:00 UTC (variables on bottom with indices 12): F. Enthalpy ($c_p T_{12}$); G. Geopotential (Φ_{12}); H. Latent heat content ($L_v q_{12}$); I. Moist static energy (MSE_{12}); J. Dry static energy (DSE_{12}). Months are on the x-axis, from January to December, and altitude on the y-axis, from 50 m to 10.0 km. The energy values are multiplied by the power 10^3 and in units of J/kg.

units of J/kg. Enthalpy reduces by approximately 90×10^3 J/kg from 50 m to 1.5 km but presents a little more concentration of energy closer to the surface during the day than at night from May to November (Figures 3A and 3F). The geopotential is minor and regular, increasing from 0 to 14×10^3 J/kg at both times (Figures 3B and 3G). Latent heat content is irregular and more concentrated at each level during the day than at night, decreasing from 36×10^3 J/kg to 23×10^3 J/kg at both times (Figures 3C and 3H).

Geopotential pointed to a regularity, unlike enthalpy, that grew into a little more in the second semester than the first semester in the year and presented a minor difference between 00:00 UTC and 12:00 UTC (Figures 3A, 3B, 3F, and 3G). Dry static energy showed a slight difference between the day and the night but was constant at both times (Figures 3E and 3J). Latent heat content presented minor variations, oscillating from January to December (Figures 3C and 3H), implying short variations and oscillations in the moist static energy (MSE_{00} and MSE_{12})

during the year (Figures 3D and 3I). Although the moist static energy was slightly different from night to day, it was generally a conserved quantity under adiabatic and hydrostatic transformations, such that a change in the latent heat content compensated for any change in enthalpy and potential energy.

Figure 4 presents the difference between 00:00 UTC and 12:00 UTC of the monthly average enthalpy ($c_p T$), geopotential (Φ), latent heat content ($L_v q$), moist static energy (MSE), and dry static energy (DSE) for the atmosphere as a Van Der Waals from 50 m to 10.0 km during the year over the MRN, where all energy values are multiplied by the power 10^3 and in units of J/kg.

Enthalpy difference exhibited a range of positive variation between 1.0 km and 2.5 km during the year, while geopotential difference showed a minor regularity, such that moist static energy difference presented the exact variability of enthalpy (Figures 4A, 4B, and 4E). Latent heat content

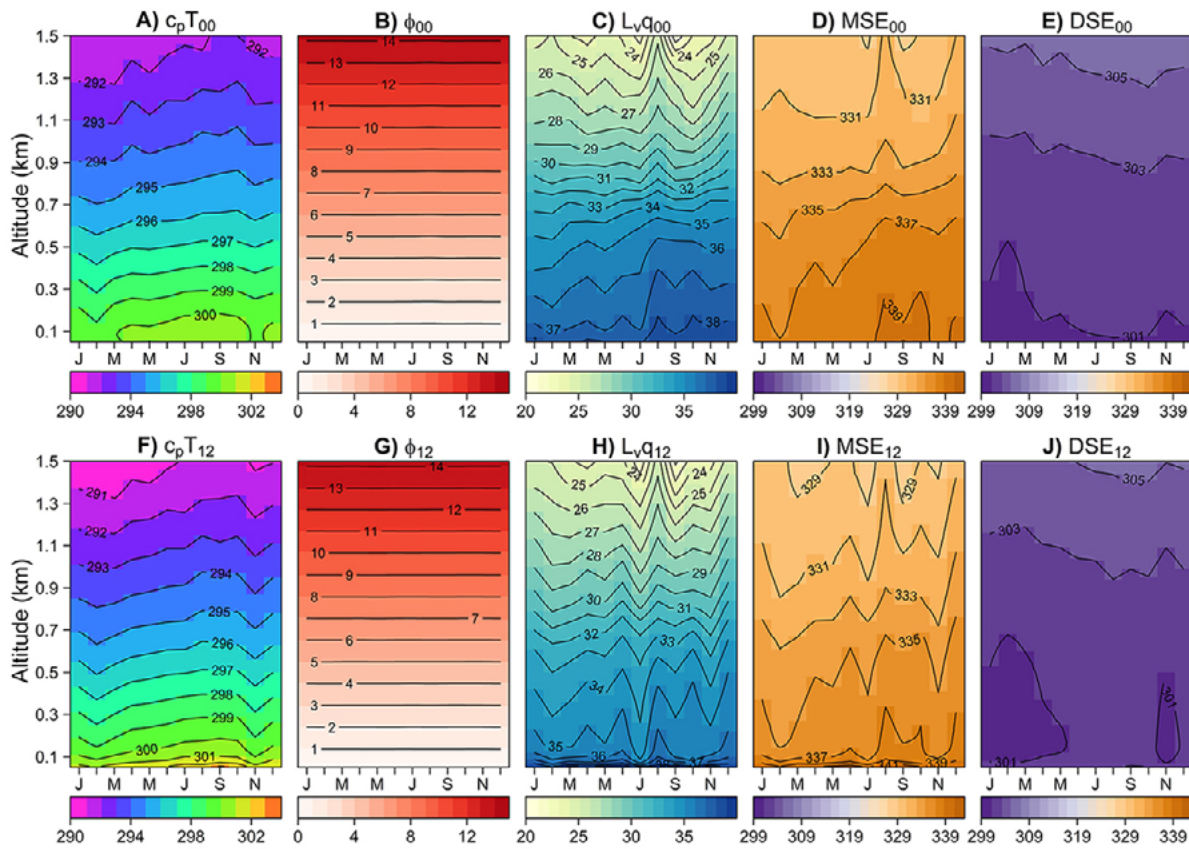


Figure 3 Vertical profiles of the atmosphere as a Van Der Waals gas for the years 2015 and 2017 over the MRN. Monthly average at 00:00 UTC (variables on top with indices 00): A. Enthalpy ($c_p T_{00}$); B. Geopotential (Φ_{00}); C. Latent heat content ($L_v q_{00}$); D. Moist static energy (MSE_{00}); E. Dry static energy. Monthly average at 12:00 UTC (variables on bottom with indices 12): F. Enthalpy ($c_p T_{12}$); G. Geopotential (Φ_{12}); H. Latent heat content ($L_v q_{12}$); I. Moist static energy (MSE_{12}); J. Dry static energy (DSE_{12}). Months are on the x-axis, from January to December, and altitude on the y-axis, from 50 m to 1.5 km. The energy values are multiplied by the power 10^3 and in units of J/kg.

difference presented a range of wide positive variations of surface to 1.0 km and chaotic positive disturbances between 1.0 km and 6.0 km during the year (Figure 4C). The night-day positive variability of enthalpy and latent heat content implied positive variations in an extent next to the surface and an array of chaotic waves in the moist static energy difference between the surface and 6.0 km during the year (Figures 4A, 4C, and 4D).

Figure 5 shows the difference between Van Der Waals atmosphere and ideal gas atmosphere for geopotential ($\Delta\Phi_{00}$ and $\Delta\Phi_{12}$, Figures 5A and 5D), moist static energy (ΔMSE_{00} and ΔMSE_{12} , Figures 5B and 5E), and dry static energy (ΔDSE_{00} and ΔDSE_{12} , Figures 5C and 5F) at 00:00 UTC and 12:00 UTC, where all energy values are in units of J/kg. The values decrease from -5 J/kg to -60 J/kg, varying between 0.002% and 0.025% of the energy quantities from the low to mid-troposphere. Therefore, the atmosphere as

an ideal gas showed approximately the same results as the Van Der Waals gas, corroborating the approach through the mathematical approximation based on the Calculus.

4 Conclusion

This work has studied the atmosphere as a system per unit mass in a Van Der Waals gas over the metropolitan region of Natal in Rio Grande do Norte, Brazil. Hence, the monthly average enthalpy, geopotential, latent heat content, moist static energy, and dry static energy were evaluated at regular altitudes, measured by the radiosonde at 00:00 UTC and 12:00 UTC for 2015 and 2017. The atmosphere as a Van Der Waals gas and the atmosphere as an ideal gas were then compared.

An unusual and innovative approach was used to compute the geopotential based on approximating the

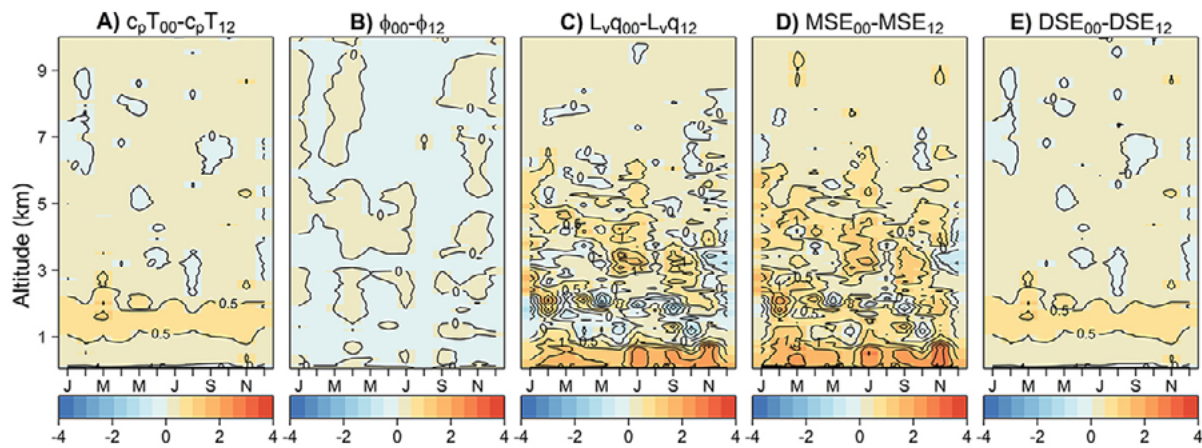


Figure 4 Difference between 00:00 UTC and 12:00 UTC of the monthly average vertical profile of the atmosphere as a Van Der Waals gas for the years 2015 and 2017 over the MRN: A. Enthalpy ($c_p T_{00} - c_p T_{12}$); B. Geopotential ($\Phi_{00} - \Phi_{12}$); C. Latent heat content ($L_v q_{00} - L_v q_{12}$); D. Moist static energy ($MSE_{00} - MSE_{12}$); and E. Dry static energy ($DSE_{00} - DSE_{12}$). Months are on the x -axis, from January to December, and altitude on the y -axis, from 50 m to 10.0 km. The energy values are multiplied by the power 10^3 and in units of J/kg.

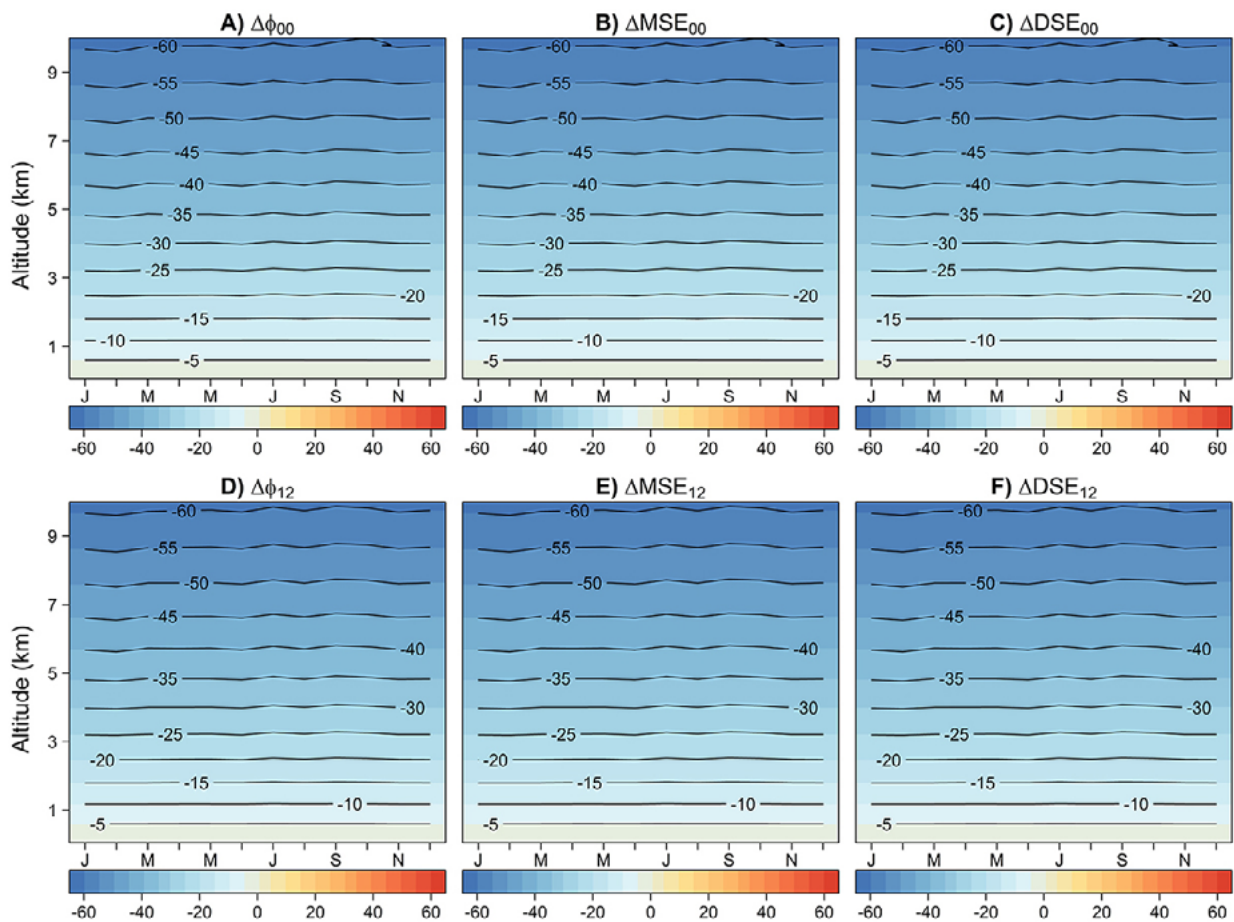


Figure 5 Difference between Van Der Waals atmosphere and ideal gas atmosphere for geopotential at 00:00 UTC and 12:00 UTC: A. $\Delta\Phi_{00}$, D. $\Delta\Phi_{12}$. Moist static energy at 00:00 UTC and 12:00 UTC: B. ΔMSE_{00} ; E. ΔMSE_{12} . Dry static energy at 00:00 UTC and 12:00 UTC: C. ΔDSE_{00} , F. ΔDSE_{12} . Months are on the x -axis, from January to December, and altitude on the y -axis, from 50 m to 10.0 km. The energy values are in units of J/kg.

definite integral from the Calculus. The nocturnal and diurnal vertical profiles of the monthly average enthalpy, geopotential, latent heat content, moist static energy, and dry static energy of a Van der Waals-like atmosphere from January to December were constructed. The outcomes of the Van der Waals-like atmosphere showed that the latent heat content compensated for any change in dry static energy (enthalpy plus potential energy) from the surface to the mid-troposphere. In general, energy was exchanged among enthalpy, geopotential, and latent heat content for the saturated air lifted dry adiabatically, showing a nearly constant moist static energy. The moist static energy was a conserved quantity under adiabatic and hydrostatic transformations, although the dry static energy was not conserved. Moist static energy includes the effects of temperature and specific humidity; however, it is equivalent to dry static energy in the upper troposphere since there is little water vapor in the flow above 6 km from January to December. Regularity in the energy values of the enthalpy and geopotential suggests uniformity in dry static energy throughout the year, while variations in latent heat content cause short decreases in moist static energy. The outcomes for the atmosphere as a Van Der Waals gas and an ideal gas were approximately the same, corroborating the approach through the mathematical approximation.

High moist static energy values indicate greater atmospheric instability, as moist static energy includes contributions from temperature (enthalpy) and humidity (latent heat). Instability is often a precursor to convective activity, leading possibly to rainfall. The vertical distribution of moist static energy, particularly high moist static energy values near the surface, suggests a favorable environment for convection and rainfall. The document notes that energy exchanges involving enthalpy and latent heat content contribute to maintaining a constant moist static energy, which supports continuous moisture availability and potential for precipitation.

It would be interesting to know if the methodology used in this work could be applied to calculate the geopotential and energy budget in regions where the atmospheric composition has a high concentration rate of a specific gas other than water vapor. This approach could also help understand the energy changes in extreme atmospheric events with high moist air concentrations and high pressure. Additionally, if its components are known, this method may be used to study the thermodynamic properties of the complex atmospheres of other planets.

5 Acknowledgments

The authors would like to thank the support from the Post Graduate Pro-Rectorate of Post-Graduate Studies of the Federal University of Rio Grande do Norte. Isamara de Mendonça Silva would like to thank the Coordination for the Improvement of Higher Education Personnel (CAPES) for the doctor's degree scholarship. This study was financed in part by the Coordenação de Aperfeiçoamento de Pessoal de Nível Superior - Brasil (CAPES) - Finance Code of the Social Demand Program: 88887.627658/2021-00.

6 References

- Alvares, C. A., Stape, J. L. & Sentelhas, P. C. 2014, 'Köppen's climate classification map for Brazil', *Meteorologische Zeitschrift*, vol. 22, n. 6, pp. 711-28.
- Bolton, D. 1980, 'The Computation of Equivalent Potential Temperature', *Monthly Weather Review*, vol. 108, pp. 1046-53.
- Chouinard, C. & Staniforth, A. 1995, 'Deriving Significant-Level Geopotentials from Radiosondes reports', *Monthly Weather Review*, vol. 123, no. 1, pp. 222-9.
- Daubert, T.E. & Bartakovits, R. 1989, 'Prediction of Critical Temperature and Pressure of Organic Compounds by Group Contribution', *Industrial and Engineering Chemistry Research*, vol. 28, no. 5, pp. 638-41.
- Ermakov, D., Kuzmin, A., Pashinov, E., Sterlyadkin, V., Chernushich, A. & Sharkov, E. 2021, 'Comparison of Vertically Integrated Fluxes of Atmospheric Water Vapor According to Satellite Radiothermography, Radiosondes, and Reanalysis', *Remote Sensing*, vol. 13, no. 9, 1639.
- Holton, J.R. 2004, *An Introduction to Dynamic Meteorology*, Elsevier Academic Press, California.
- Huang, P. 2018, 'A Simple Accurate Formula for Calculating Saturation Vapor Pressure of Water and Ice', *Journal of Applied Meteorology and Climatology*, vol. 57, no. 6, pp. 1265-72.
- IBGE 2021, *Censo Nacional. Instituto Brasileiro de geografia e Estatística*, <<https://www.ibge.gov.br/en/cities-and-states/rn/natal.html>>.
- Internet Archive 2010, *WayBackMachine*, <<https://web.archive.org/web/20101009044345/>>.
- Jalowka, J.W. & Daubert, T.E. 1986, 'Group Contribution Method to Predict Critical Temperature and Pressure of Hydrocarbons', *Industrial & Engineering Chemistry Research*, vol. 25, no. 1, pp. 139-142.
- Joback K.G. & Reid, R.C. 1987, 'Estimation of Pure-Component Properties from Group Contributions', *Chemical Engineering Communications*, vol. 57, no. 1-6, pp. 233-43.
- Kay, W.B. 1936, 'Gases and Vapors At High Temperature and Pressure - Density of Hydrocarbon', *Industrial and Engineering Chemistry*, vol. 28, no. 9, pp. 1014-9.
- Laroche, S. & Sarrazin, R. 2013, 'Impact of Radiosonde Balloon Drift on Numerical Weather Prediction and Verification', *Weather and Forecasting*, vol. 28, no. 3, pp. 772-82.

- Marshall, G.J. 2002, 'Trends in Antarctic Geopotential Height and Temperature: A Comparison between Radiosonde and NCEP – NCAR Reanalysis Data', *Journal of Climate*, vol. 15, no. 6, pp. 659-74.
- Medeiros, D.M., Silva, I.M., Silva, D.N. & Mendes, D. 2020, 'Van der Waals-like State Equation for Atmosphere', *Anuário do Instituto de Geociências*, vol. 43, no. 2, pp. 55-63.
- NASA – National Aeronautics and Space Administration 2021, *Earth Fact Sheet*, Washington DC, <<http://nssdc.gsfc.nasa.gov/planetary/factsheet/earthfact.html>>.
- Nussenzweig, H.M. 2000, *Curso de Física Básica: 2 - Fluidos, Oscilações e Ondas, Calor*, Editora Edgard Blücher LTDA, São Paulo.
- Qian, X., Yao, Y., Wang, H., Wang, Y., Bai, Z. & Yin, J. 2018, 'The Characteristics at the Ali Observatory Based on Radiosonde Observations', *Publications of the Astronomical Society of the Pacific*, vol. 130, no. 994, 125002.
- Rogers, R.R. & Yau, M.K. 1996, *A Short Course in Cloud Physics*, Butterworth Heinemann/Elsevier Science, Saint Louis.
- Silva, I.M., Silva, D.N. & Medeiros, D.M. 2019, 'Vertical Profile of Density in a Van Der Waals Atmosphere in Natal City', *Holos*, vol. 2, pp. 1-10.
- Smith, W.L., Woolf, H.M. & Jacob, W.J. 1970, 'A Regression Method for Obtaining Real-Time Temperature and Geopotential Height Profiles from Satellite Spectrometer Measurements and its Application to Nimbus 3 "Sirs" Observations', vol. 98, no. 8, pp. 582-603.
- Stewart, J. 2016, *Calculus*, Cengage Learning, Boston.
- Tetens, V.O. 1930, 'Über einige meteorologische Begriffe', *Zeitschrift Geophysic*, Wurzburg, vol. 6, pp. 297-309.
- Wallace, J.M. & Hobbs, P.V. 2006, *Atmospheric Science - An Introductory Survey*, Elsevier Academic Press, San Diego.
- Van der Waals, J.D. 1873, 'On the Continuity of the Gaseous and Liquid States, Doctoral Dissertation, Leiden University, Leiden, Netherland.
- Zhang, Y. & Fueglistaler, S. 2020, 'How tropical convection couples high moist static energy over land and ocean', *Geophysical Research Letters*, 47, e2019GL086387, <<https://doi.org/10.1029/2019GL086387>>.
- Yano, J.I. & Ambaum, M.H.P. 2017, 'Moist static energy: Definition, reference constants, a conservation law and effects on buoyancy', *Quarterly Journal of the Royal Meteorological Society*, vol. 143, no. 708, pp. 2727-34, <<https://rmets.onlinelibrary.wiley.com/doi/abs/10.1002/qj.3121>>.

Author contributions

Deusdedit Monteiro Medeiros: conceptualization; formal analysis; methodology; writing-original draft; writing - review and editing; visualization; supervision. **Isamara de Mendonça Silva:** conceptualization; formal analysis; methodology; writing - review and editing; visualization. **David Mendes:** writing - review and editing.

Conflict of interest

The authors declare no potential conflict of interest.

Data availability statement

All data included in this study are publicly available in the Wyoming Weather Web dataset of The Department of Atmospheric Science of the College of Engineering and Physical Sciences of the University of Wyoming (<https://weather.uwyo.edu/upperair/sounding.html>).

Funding information

Not applicable.

Editor-in-chief

Dr. Claudine Dereczynski

Associate Editor

Dr. Fernanda Cerqueira Vasconcellos

How to cite:

Medeiros, D.M., Silva, I. de M. & Mendes, D. 2025, 'Assessing the Moist and Dry Static Energies in the Atmosphere as a Van Der Waals Gas in 2015 and 2017 over the Metropolitan Region of Natal-RN, Brazil' *Anuário do Instituto de Geociências*, 48:62091. https://doi.org/10.11137/1982-3908_2025_48_62091

